

Article

Spin-Polarized Photoelectron Fluxes from Fullerene Anions

Valeriy K. Dolmatov Department of Physics and Earth Science, University of North Alabama, Florence, AL 35630, USA;
vkdolmatov@una.edu

Received: 30 July 2020; Accepted: 24 September 2020; Published: 29 September 2020



Abstract: Initial insights into spin-polarized photoelectron fluxes from fullerene anions are presented here. Both the angle-dependent and angle-integrated degrees of spin polarization of said photoelectron fluxes are discussed. Empty $C_{60}^-(2p)$ and endohedral $H@C_{60}^-(2p)$ and $He@C_{60}^-(2p)$ anions, where the attached electron resides in a $2p$ state, are chosen as case studies. We uncover the characteristics of the phenomenon in the framework of a semi-empirical methodology where the C_{60} cage is modeled by a spherical annular potential, rather than aiming at a rigorous study. It is found that the spin-polarization degree of photoelectron fluxes from fullerene anions can reach large values, including a nearly complete polarization, at/in specific values/domains of the photoelectron momentum. This is shown to correlate with an inherent feature of photoionization of fullerenes, the abundance of resonances, known as confinement resonances, in their photodetachment spectra owing to a large empty space inside fullerenes. Moreover, the results obtained can serve as a touchstone for future studies of the phenomenon by more rigorous theories and/or experiments to reveal the significance of interactions omitted in the present study.

Keywords: spin-polarization; fullerene anions; endohedral fullerene anions; photodetachment

1. Introduction

Photoionization/photodetachment of various neutral ($q = 0$) and charged ($q \neq 0$) fullerenes, $C_N^{\pm q}$, and their endohedral counterparts, $A@C_N^{\pm q}$ (where A is the atom encapsulated inside $C_N^{\pm q}$ cage), has been the subject of experimental as well as intense systematic theoretical studies for many years now, see, e.g., [1–24] (and references therein). However, the subject of spin-polarized photoelectron fluxes from fullerene anions (or neutral $A@C_N$, for that matter) was provisionally touched briefly only in [25,26], to the best of the author's knowledge. Meanwhile, fundamentally, the topic of spin-polarized electron beams is of significance to both basic and applied sciences [27]. The present paper remedies the situation by producing novel results and findings related to spin-polarized photoelectron fluxes from fullerene anions.

We investigate and predict peculiarities in spin-polarized photoelectron fluxes upon photodetachment of a $C_{60}^-(2p)$ fullerene, where an external electron is captured into a $2p$ -state in the field of the C_{60} cage.

Moreover, with the impetus of work [15], where it was predicted that the embedded into a neutral C_{60} fullerene cage atom, A , can qualitatively modify the photoionization spectrum of the C_{60} cage itself, we study how the photodetachment properties of fullerene anions can be affected by the embedded atom inside a hollow interior of $C_{60}^-(2p)$. Such systems are referred to as $A@C_{60}^-(2p)$ endohedral fullerene anions. We choose the $H@C_{60}^-(2p)$ and $He@C_{60}^-(2p)$ endohedral anions for case studies and demonstrate how their photodetachment parameters differ from those of the empty $C_{60}^-(2p)$.

Furthermore, we investigate how accounting for polarization of the fullerene cage by the outgoing photoelectron affects the spin polarization degree of the emitted photoelectrons.

The culmination point of the the present work is the prediction that photodetachment of fullerene anions can serve as a tool for the production of highly spin-polarized electron beams.

The present paper, thus, provides a broad initial investigation into spin-polarized photoelectron fluxes from fullerene anions, albeit being carried out within a simple (semi-)empirical model. The latter is similar in its spirit to the (semi-)empirical model originally suggested in [4] and later in [5] for studying of photodetachment of $C_{60}^-(n\ell)$. There, the C_{60} cage was modeled by an infinitesimally thin Dirac-bubble potential, $U(r) = A\delta(r - r_C)$ (r_C is the radius of the C_{60} skeleton) which binds an external electron into a $n\ell$ state, thereby turning C_{60} into a $C_{60}^-(n\ell)$ fullerene anion. A more realistic model, however, must account for a finite thickness of the fullerene cage. This is exactly what we do in the present paper. Namely, we model the C_{60} cage by a spherical annular potential of a certain inner radius, r_{in} , and finite thickness, Δ . This is because such model has been proven [18,20,28,29] (and references therein) to produce results in a reasonably good agreement with both the experimental photoionization spectrum of endohedral $Xe@C_{60}^+$ [20] and differential elastic electron scattering off C_{60} [30], particularly when polarization of the C_{60} cage by the outgoing photoelectron was accounted by theory [18,28,29]. Such modeling was also shown [31] to result in a semi-quantitative agreement with some of the most prominent features of the $e^- - C_{60}$ total elastic electron scattering cross section predicted by a far more sophisticated ab initio molecular-Hartree-Fock approximation. Thus, in the present paper, we utilize the described model, combine it with Cherepkov's theory [32,33] of spin-polarized photoelectron fluxes from atomic targets, and demonstrate that the emitted photoelectrons from fullerene anions can have a high degree of spin polarization.

It is clear that, of course, photodetachment of a fullerene anion is a much more complicated process than the simplified model suggests. It is a multifaceted problem. It presents a challenge to theory. In the present work, we peel off only a "facet" related to the inherent geometry of C_{60} to learn if there is something worthy of attention hidden behind the "facet", instead of performing rigorous high-level calculations of the phenomenon. One of a higher-level study could be the investigation of the impact of the surface and volume plasmons photoexcited in a fullerene anion by the incoming electromagnetic radiation, as in the case of photoionization of positive fullerene ions [13]. These plasmon excitations can induce a rather strong collective effect in about $\hbar\omega = 10$ to 50 eV domain of the photon energy. However, as is discussed in the end of Section 2.2 of the paper, the binding energy, E_{2p} , of a $2p$ attached electron in $C_{60}^-(2p)$, $H@C_{60}^-(2p)$ and $He@C_{60}^-(2p)$ is approximately -2.65 eV. Therefore, the plasmon effect on photodetachment of these fullerene anions should start matter at the photoelectron momenta $k = \sqrt{2(\hbar\omega + E_{2p})} \geq 0.7$ a.u. Thus, in the range of k 's up to $k \approx 0.7$ a.u. one can reasonably expect that the utilized in the present work model is usable, to a good approximation. Furthermore, as will be shown below, the spin-polarization characteristics of the ejected photoelectrons depend on the $\frac{d_{\ell-1}}{d_{\ell+1}}$ ratio of the $d_{\ell-1}$ and $d_{\ell+1}$ dipole photodetachment amplitudes. This might result in a partial cancelation of the plasmon effects and, thus, in their weakened impact on the spin-polarization parameters of the ejected photoelectrons. Therefore, one can reasonably expect that the model is still usable for studying spin-polarized fluxes of photoelectrons even at the values of $k > 0.7$ a.u. Anyway, such calculated results are needed to reveal a role of collective effects in the subject of study that would remain undetermined otherwise. Accounting for collective effects themselves is beyond the scope of the present paper. As such, the present study may be the impetus for future rigorous theoretical or experimental studies of the phenomenon.

In addition, the present study also carries an alternative significance regardless of its relevance to fullerene anions. It relates to a topic of the structure and spectra of confined quantum systems in whole. To date, confined systems have been scrutinized intensely worldwide by exploiting various sorts of imaginable external confinements [34–41] (and references therein). As a perspective, the present work, too, contributes something new to the knowledge box on confined quantum systems in general.

Atomic units (a.u.) are used throughout the text, assuming the electronic charge $|e^-|$, mass m and Planck's constant \hbar are equal to unity: $|e^-| = m = \hbar = 1$.

2. Review of Theory

2.1. Cherepkov's Theory of Spin-Polarized Photoelectron Fluxes from Atoms

To date, theory and experiment on the production of spin-polarized electrons have been developed to a high degree [27,32,33,42] (and references therein).

In the present paper, we follow Cherepkov's work [32,33] on spin-polarized photoelectron fluxes upon photoionization of a $n\ell$ -subshell ($\ell \geq 1$) of an unpolarized atom. We focus on the simplest case of theory. Namely: (a) A photoionized $n\ell_j$ atomic subshell is a single-electron subshell having the definite total angular momentum j , $j = \ell \pm \frac{1}{2}$, (b) a photon flux is circularly-polarized and it is propagating along the Z-axis of the XYZ coordinate system, (c) the photoelectron has a definite spin projection, $\mu = \pm \frac{1}{2}$, on the Z axis. The corresponding differential photoionization cross section, $\frac{d\sigma_j}{d\Omega} \equiv I_j(\omega, \theta, \mu)$, by a right-hand circularly-polarized photon is [32]:

$$I_j(\omega, \theta, \mu) = \frac{\sigma_{\text{tot}}^j(\omega)}{8\pi} \left\{ 1 + A_j(\omega)\text{sign}\mu - \left[\frac{1}{2}\beta(\omega) + \gamma_1(\omega)\text{sign}\mu \right] P_2(\cos\theta) \right\}. \quad (1)$$

Here, $P_2(\cos\theta)$ is a Legendre polynomial, θ is the photoelectron emission angle relative to the Z axis, σ_{tot}^j is the photoionization cross section of a $n\ell_j$ ($\ell \geq 1$) single-electron outer subshell of the atom, $\beta(\omega)$ is the well-known angular-asymmetry parameter of the photoelectron angular distribution, and $A_j(\omega)$ and $\gamma_1(\omega)$ are spin-polarization parameters [32]:

$$\beta = \frac{\ell(\ell-1)d_{\ell-1}^2 + (\ell+1)(\ell+2)d_{\ell+1}^2 - 6\ell(\ell+1)d_{\ell-1}d_{\ell+1}\cos(\delta_{\ell+1} - \delta_{\ell-1})}{(2\ell+1)[\ell d_{\ell-1}^2 + (\ell+1)d_{\ell+1}^2]}, \quad (2)$$

$$A_j = (-1)^{j-\ell-\frac{1}{2}} \frac{\ell(\ell+1)(d_{\ell+1}^2 - d_{\ell-1}^2)}{(2j+1)[\ell d_{\ell-1}^2 + (\ell+1)d_{\ell+1}^2]}, \quad (3)$$

$$\gamma_1 = (-1)^{j-\ell-\frac{1}{2}} \frac{2\ell(\ell+1)[(\ell+2)d_{\ell+1}^2 - (\ell-1)d_{\ell-1}^2 + 3d_{\ell-1}d_{\ell+1}\cos(\delta_{\ell+1} - \delta_{\ell-1})]}{(2j+1)(2\ell+1)[\ell d_{\ell-1}^2 + (\ell+1)d_{\ell+1}^2]}, \quad (4)$$

$$d_{\ell\pm 1} = \int_0^\infty r^2 R_{n\ell}(r) R_{\ell\pm 1}(r) dr. \quad (5)$$

Here, $d_{\ell\pm 1}$ are the radial parts of the photoionization amplitudes for the ejection of an $n\ell$ -electron into $\epsilon, \ell \pm 1$ continuum spectra, ϵ is the kinetic energy of the photoelectron, $R_{n\ell}(r)$ and $R_{\epsilon, \ell\pm 1}(r)$ are the radial parts of the corresponding wavefunctions of the initial and final states, $\delta_{\ell\pm 1}$ are phases of the photoelectron wavefunctions.

The angular dependence of the the spin-polarization degree of a photoelectron flux, $P_j(\theta)$, is defined [32] as

$$P_j(\theta) = \frac{I_j(\theta, \frac{1}{2}) - I_j(\theta, -\frac{1}{2})}{I_j(\theta, \frac{1}{2}) + I_j(\theta, -\frac{1}{2})} = \frac{A_j - \gamma_1 P_2(\cos\theta)}{1 - \frac{1}{2}\beta P_2(\cos\theta)}. \quad (6)$$

The total, i.e., angle-integrated degree of the photoelectron spin polarization, P_j , is obtained by the integration, separately, of the numerator and denominator of Equation (6) with respect to the solid angle, $d\Omega$. As a result, one finds [32] that P_j is the same as the A_j parameter, Equation (3):

$$P_j = A_j \tag{7}$$

The most interesting and important situation for getting strongly spin-polarized photoelectron fluxes, is when (a) a normally inferior transition, $d_{\ell-1}$, turns into a dominant transition compared to a normally superior transition, $d_{\ell+1}$, i.e., when $d_{\ell-1} > d_{\ell+1}$, and (b) a photoionized atomic subshell is a np -subshell ($\ell = 1$) with the total angular momentum $j = \ell - \frac{1}{2} = \frac{1}{2}$. Indeed, when $d_{\ell-1} > d_{\ell+1}$, Equations (3) and (7) say [32]:

$$P_{j=\ell-\frac{1}{2}} \Big|_{d_{\ell-1} > d_{\ell+1}} \leq \frac{\ell+1}{2\ell} \Big|_{\ell=1} \leq 1 \text{ and } P_{j=\frac{1}{2}} \Big|_{d_{\ell-1} \gg d_{\ell+1}} \approx 1, \text{ whereas } P_{j=\ell+\frac{1}{2}} \leq \frac{1}{2}. \tag{8}$$

In other words, photoionization of a $np_{\frac{1}{2}}$ subshell may result in an almost completely spin-polarized photoelectron flux, $P_{\frac{1}{2}} \approx 1$, regardless of the angle of emission of a $np_{\frac{1}{2}}$ -photoelectron, when $d_{\ell-1} \gg d_{\ell+1}$. It is precisely for this reason that, in the present paper, we choose fullerene anions where the attached electron is a $p_{\frac{1}{2}}$ -electron and study the phenomenon of spin-polarized photoelectron fluxes upon $p_{\frac{1}{2}}$ -photodetachment.

2.2. Modeling Fullerene Anion Photodetachment

As mentioned above, we model (replace) the C_{60} cage by a $U_C(r)$ spherical annular potential of the inner radius, r_{in} , finite thickness, Δ , and depth, U_0 , as in many other studies, e.g., [8–11,18,20,21,28,29] (and references therein):

$$U_C(r) = \begin{cases} -U_0, & \text{if } r_{in} \leq r \leq r_{in} + \Delta \\ 0 & \text{otherwise.} \end{cases}$$

A $C_{60}^-(n\ell)$ anion, then, is formed by binding of an external electron into a $n\ell$ state by the $U_C(r)$ potential. This model of a fullerene anion is similar in its spirit to modeling C_{60} by the Dirac-bubble potential [4,5]. Next, we expand our model for $C_{60}^-(n\ell)$ to an $A@C_{60}^-$ endohedral anion, simply by positioning the A atom at the center of the $U_C(r)$ potential. Furthermore, we complete our model of fullerene anions by an approximate accounting for polarization of C_{60} by the outgoing photoelectron. Generally, this is a too complicated task to be approached rigorously as, e.g., in work [43] (and references therein) on photodetachment of free atomic anions. However, it is not the aim of the present work to develop a rigorous theory (model). Instead, we focus on gaining the first meaningful insight into the subject of study. Thus, the C_{60} polarization potential is approximated by a semi-empirical static dipole polarization potential, $V_\alpha(r)$, as in [18,28,29] (and references therein):

$$V_\alpha(r) = -\frac{\alpha}{2(r^2 + b^2)^2}. \tag{9}$$

Here, α is the static dipole polarizability of C_{60} ($\alpha \approx 850$ a.u. [44]), and b is a free parameter of the order of the fullerene size. Such accounting for polarization of C_{60} by the outgoing photoelectron has recently been proven to result in a reasonable agreement between calculated angle-differential elastic electron scattering off C_{60} [28,29] and experiment [30], as well as between the calculated [18] photoionization cross section of $Xe@C_{60}$ and experiment [20].

Thus, the total model Hamiltonian, $\hat{H}(r)$, for the bound and continuum states of the $C_{60}^-(n\ell)$ and $A@C_{60}^-(n\ell)$ anions is as follows:

$$\hat{H}(r) = U_C(r) + \hat{H}^{HF} + V_\alpha(r). \tag{10}$$

Here, \hat{H}^{HF} is the Hartree-Fock Hamiltonian of the system “encapsulated A atom plus an external electron”.

Correspondingly, the bound energy, $E_{n\ell}$, and the radial part, $P_{n\ell}(r)$, of the wavefunctions of the attached $n\ell$ electron, or its continuum-state wavefunction, $P_{\ell}(r)$, are the solutions of the following radial equation:

$$-\frac{1}{2} \frac{d^2 P_{n/\ell}}{dr^2} + \left[\frac{\ell(\ell+1)}{2r^2} + \hat{\mathcal{H}}(r) \right] P_{n/\ell}(r) = E_{n/\ell} P_{n/\ell}(r). \quad (11)$$

Here,

$$P_{n\ell}(r)|_{r \rightarrow 0, \infty} = 0, \text{ whereas } P_{\ell}(r)|_{r \gg 1} \rightarrow \sqrt{\frac{2}{\pi}} \sin \left(kr - \frac{\pi\ell}{2} + \delta_{\ell}(\epsilon) \right), \quad (12)$$

where $\delta_{\ell}(\epsilon)$ is the phase of the continuum state wavefunction and k is the photoelectron momentum.

Lastly, when solving Equation (11), we use the following values for the model adjustable parameters of the $U_C(r)$ potential: $r_{\text{in}} \approx 5.8$, $\Delta \approx 1.9$, $U_0 \approx 0.302$ and $b \approx 8$ a.u. This is because these values of the parameters were shown earlier to result in a reasonably good agreement between calculated [18,28,29] and experimental data on both elastic electron scattering off C_{60} [30] and photoionization of $\text{Xe}@C_{60}^+$ [20]. A would-be drawback of this potential regarding its application to $2p$ photodetachment of a $C_{60}^-(2p)$ anion is that it produces a $2p$ state bound by approximately -2 eV versus the known value of the -2.65 eV of electron affinity of C_{60} [45]. If we adjust U_0 to produce a $2p$ state bound by -2.65 eV, then $U_0 = 0.347$ a.u. The question, then, is whether the use of $U_0 = 0.302$ a.u. is justified for the present study. We have carefully analyzed this situation by performing parallel calculations for a $C_{60}^-(2p)$ anion (i.e., one with the use of $U_0 = 0.302$ a.u. and the other one with the use of $U_0 = 0.347$ a.u.). Namely, we calculated the corresponding P_{2p} radial wavefunction, $\sigma_{2p \rightarrow s}$ and $\sigma_{2p \rightarrow d}$ partial photodetachment cross sections, β_{2p} photoelectron angular-asymmetry parameter, γ_1 spin-polarization parameter as well as the $A_1 = P_{j=\frac{1}{2}}$ spin-polarization degree of ejected photoelectrons. Moreover, the stated calculations were performed with and without account for polarization of C_{60} by the outgoing photoelectron. Calculated data are presented in the Appendix A. They show that there is a negligible difference in the $P_{2p}(r)$ radial functions of a $2p$ bound-state between the two calculated sets of data. Likewise, there are only insignificant differences between the photodetachment characteristics, plotted versus the photoelectron momentum, $k = \sqrt{2(\hbar\omega + E_{2p})}$, calculated with the use of both potentials. Because of a semi-quantitative nature of the present study, these insignificant differences can hardly matter at all. More so, when polarization of C_{60} by the outgoing photoelectron is considered, there is practically no difference in $\sigma_{2p \rightarrow s}$, $\sigma_{2p \rightarrow d}$, β_{2p} , γ_1 and $A_1 = P_{j=\frac{1}{2}}$ between the two sets of calculated data plotted versus k . In terms of the photon energy, “competing” graphs obtained with the use of $U_0 = 0.302$ a.u. can simply be shifted by 0.65 eV to match the threshold of $E_{2p} = -2.65$ eV, if wanted. Therefore, it does not, actually, matter which of the two values of U_0 to use to proceed with the planned study. We prefer to operate with $U_0 \approx 0.302$ a.u., for the sake of consistency with a series of our former calculations. This is more so, because such defined $U_C(r)$ pseudo-potential led us previously to a reasonable agreement between calculated and experimental data on photoionization of $\text{Xe}@C_{60}^+$ and elastic electron scattering off C_{60} , as was mentioned above. Moreover, we plot calculated photodetachment parameters versus the photoelectron momentum k , because it eliminates the necessity to know the exact value of the E_{2p} binding energy.

3. Results and Discussion

Let us first get a quantitative information about the one-electron configurations of the $C_{60}^-(2p)$, $\text{H}@C_{60}^-(2p)$ and $\text{He}@C_{60}^-(2p)$ anions. To do so, let us utilize Equation (11), where we exclude the V_{α} polarization potential. This is because V_{α} is irrelevant to the ground-states of the anions. Calculated

radial functions of the attached $2p$ electron, $P_{2p}(r)$, as well as the $1s$ radial functions, $P_{1s}(r)$, of the encapsulated H and He atoms are plotted in Figure 1.

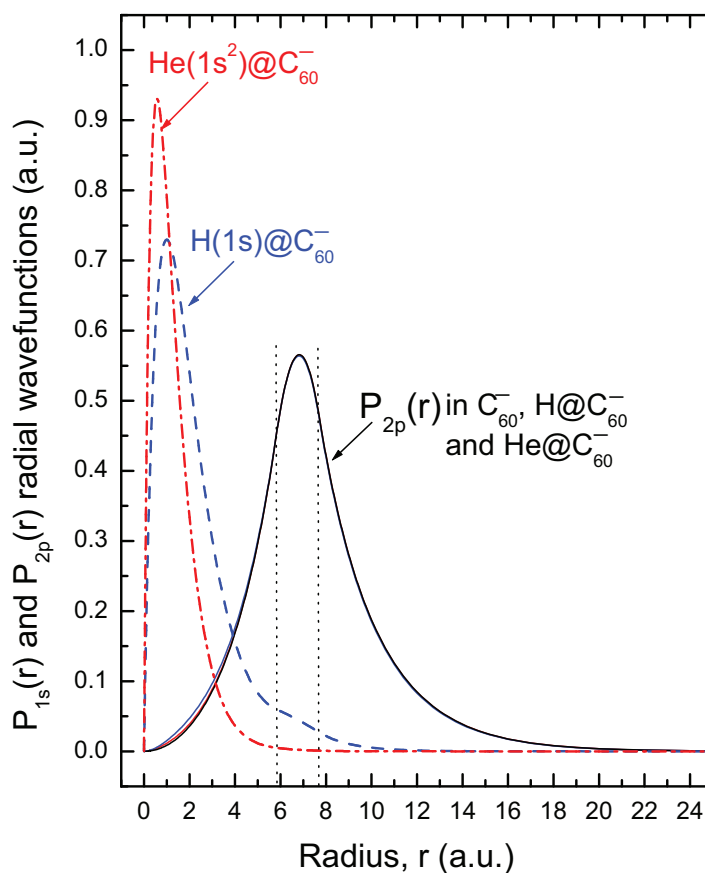


Figure 1. Calculated $P_{1s}^H(r)$ and $P_{1s}^{He}(r)$ radial functions of the encapsulated H and He atoms, as well as the $P_{2p}(r)$ radial function of the attached $2p$ -electron in the $C_{60}^-(2p)$, $H@C_{60}^-(2p)$ and $He@C_{60}^-(2p)$ fullerene anions, as marked. Note: the $P_{2p}(r)$ functions in these anions are practically indistinguishable from one another. Vertical dotted lines mark the boundaries of the C_{60} shell.

Note how the calculated bound $P_{2p}(r)$ functions in these anions are practically indistinguishable from one another with an insignificant exception at small r 's. Hence, if one to expect differences in photoionization characteristics between these anions, they will be due to the differences between the electron densities affecting the photoelectron wave primarily inside the hollow interior of C_{60} .

Calculated $\sigma_{2p \rightarrow s}$ and $\sigma_{2p \rightarrow d}$ partial photodetachment cross sections of $C_{60}^-(2p)$, $H@C_{60}^-(2p)$ and $He@C_{60}^-(2p)$ are depicted in Figure 2.

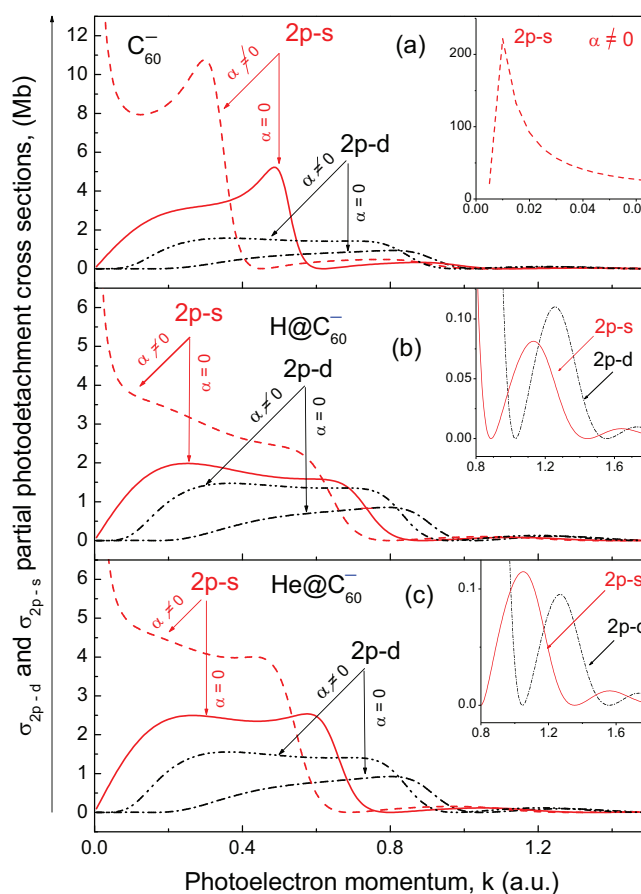


Figure 2. Partial $\sigma_{2p \rightarrow s}$ and $\sigma_{2p \rightarrow d}$ photodetachment cross sections of (a) $C_{60}^{-}(2p)$, (b) $H@C_{60}^{-}(2p)$ and (c) $He@C_{60}^{-}(2p)$ calculated without account ($\alpha = 0$) and with account ($\alpha \neq 0$) for polarization of the fullerene anions by the outgoing photoelectron, as marked. Inserts: $\sigma_{2p \rightarrow s}$ and $\sigma_{2p \rightarrow d}$ plotted on an extended k -scale, as marked.

Firstly, which is of primary importance to the present paper, one can see that $\sigma_{2p \rightarrow s}$ exceeds considerably $\sigma_{2p \rightarrow d}$ in the interval of k from threshold to several tenths' a.u. Then, again, $\sigma_{2p \rightarrow s} \gg \sigma_{2p \rightarrow d}$, at selected higher values of k . The latter is because $\sigma_{2p \rightarrow s}$ is oscillating, resonantly, in anti-phase relative to the oscillating $\sigma_{2p \rightarrow d}$, as is clearly demonstrated in inserts in Figure 2b,c. Note, resonance oscillations in $\sigma_{2p \rightarrow s}$ and $\sigma_{2p \rightarrow d}$ emerge at lower values of k as well, albeit they are less sharp. For C_{60}^{-} , the resonance oscillations in $\sigma_{2p \rightarrow s}$ and $\sigma_{2p \rightarrow d}$ were first uncovered in [4] and re-discovered in [5]. They are similar in nature to resonances that have been extensively scrutinized in photoionization of the A atom of $A@C_{60}$ endohedral fullerenes for some time now, see, e.g., [8,11,12,14,18–24] (and references therein). The resonances are due to the interference of the photoelectron waves scattered off the inner and outer walls of the C_{60} cage. Following [46], these resonances are commonly referred to as the confinement resonances. The demonstrated fact that $\sigma_{2p \rightarrow s}$ can considerably exceed $\sigma_{2p \rightarrow d}$ not only when $\sigma_{2p \rightarrow d}$ is nearly a zero at the resonance minima, but also when $\sigma_{2p \rightarrow d}$ is fairly large (at lower values of k), is an outstanding feature of the photodetachment of fullerene anions. It is precisely because of this feature that fullerene anions can serve as new sources of highly spin-polarized electron beams, as will soon be shown in the present paper.

Secondly, note how $\sigma_{2p \rightarrow s}$ and $\sigma_{2p \rightarrow d}$ of $H@C_{60}^{-}(2p)$ and $He@C_{60}^{-}(2p)$ differ from those of empty $C_{60}^{-}(2p)$. We attribute this primarily to the additional scattering of the photoelectron wave off the encapsulated atom inside C_{60} compared to the case of empty $C_{60}^{-}(2p)$. Thus, the photodetachment

parameters of fullerene anions can be tailored to one's needs by encapsulating an atom inside the C_{60}^- cage.

Thirdly, one can see that accounting for polarization of the fullerene anions by the outgoing photoelectron affects strongly both the magnitudes and k -dependence of $\sigma_{2p \rightarrow s}$ and $\sigma_{2p \rightarrow d}$. Especially strong changes are incurred by the polarization effect to $\sigma_{2p \rightarrow s}$ at low photoelectron momenta. Very near the threshold the changes are dramatic, resulting in an extremely narrow resonance in $\sigma_{2p \rightarrow s}$. The latter is depicted in insert in Figure 2a, for C_{60}^- .

The angle-integrated degrees of the photoelectron spin polarization, $P_{j=\frac{1}{2}}$, upon photodetachment of $C_{60}^-(2p)$, $H@C_{60}^-(2p)$ and $He@C_{60}^-(2p)$, calculated without ($\alpha = 0$) and with ($\alpha \neq 0$) account for polarization of the C_{60} cage by the outgoing photoelectron, are depicted in Figure 3.

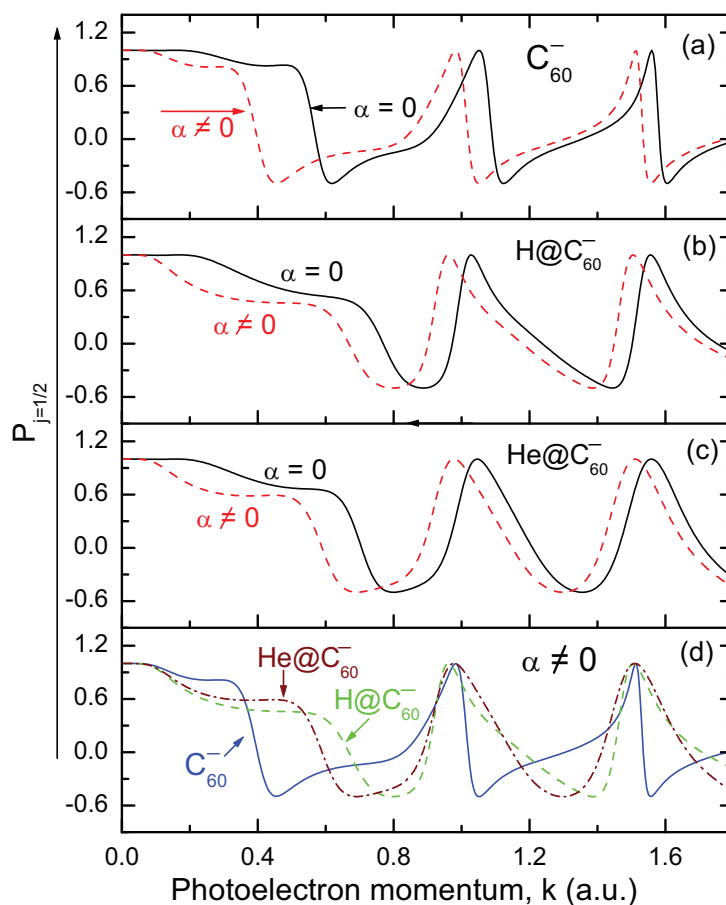


Figure 3. The angle-integrated degree of photoelectron spin polarization, $P_{j=\frac{1}{2}}$, upon photodetachment of the fullerene anions calculated without account ($\alpha = 0$) and with account ($\alpha \neq 0$) for polarization of the C_{60} cage by the outgoing photoelectron, as marked. (a) $P_{j=\frac{1}{2}}$ for $C_{60}^-(2p)$. (b) $P_{j=\frac{1}{2}}$ for $H@C_{60}^-(2p)$. (c) $P_{j=\frac{1}{2}}$ for $He@C_{60}^-(2p)$. (d) Calculated $P_{j=\frac{1}{2}}$ s for $C_{60}^-(2p)$, $H@C_{60}^-(2p)$ and $He@C_{60}^-(2p)$ graphed on the same plot to ease the comparison between them.

Owing to the fact that $\sigma_{2p \rightarrow s}$ exceeds, considerably, $\sigma_{2p \rightarrow d}$ at/in specific values/domains of k , the $P_{j=\frac{1}{2}}$ degree reaches large values in there, including the value of $P_{j=\frac{1}{2}} \approx 1$. This is in accordance with Cherepkov's theory, Equation (8). The resonances in $P_{j=\frac{1}{2}}$ are due to confinement resonances in the $2p \rightarrow d$ and $2p \rightarrow s$ photodetachment amplitudes. Next, note how accounting for the polarizability of C_{60} results in decreasing the value of $P_{j=\frac{1}{2}}$ in a domain of k 's from threshold to about 0.5 a.u. Lastly, note (see Figure 3d) how the encapsulation of an atom A into the $C_{60}^-(2p)$ cage generally broadens

the domains of k 's where $P_{j=\frac{1}{2}}$ is large. Thus, in principle, spin-polarized photoelectron fluxes from fullerene anions can be controlled, to some extent, by embedding an atom into the C_{60}^- cage.

To calculate the angular dependence of the spin-polarization degree, $P_j(\theta)$, of the photoelectron fluxes from fullerene anions, one needs to know the angular-asymmetry parameters, γ_1 and β in addition to $A_j = P_j$. Calculated γ_1 and β are depicted in Figure 4.

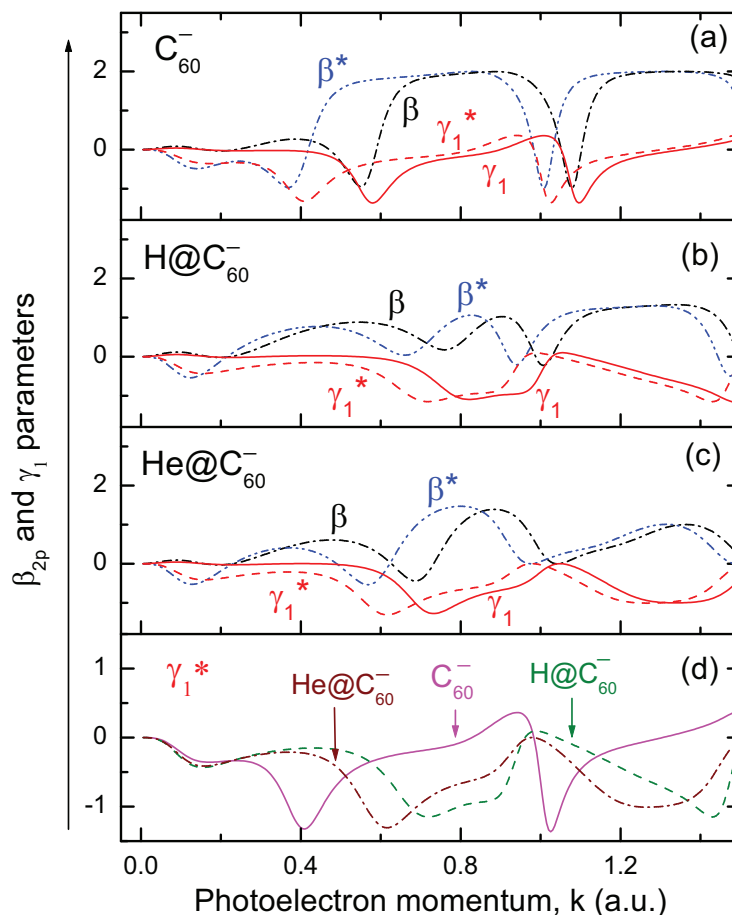


Figure 4. Calculated γ_1 and β photoelectron angular-asymmetry parameters upon $2p$ -photodetachment of (a) $C_{60}^-(2p)$, (b) $H@C_{60}^-(2p)$ and (c) $He@C_{60}^-(2p)$, as marked. Labels: γ_1/γ_1^* and β/β^* are calculated data without/with account for polarizability of C_{60} , respectively. (d) Calculated γ_1^* for $C_{60}^-(2p)$, $H@C_{60}^-(2p)$ and $He@C_{60}^-(2p)$ graphed on the same plot to ease the comparison between them.

Similar to $\sigma_{2p \rightarrow s}$, $\sigma_{2p \rightarrow d}$ and $P_{j=\frac{1}{2}}$, the angular-asymmetry parameters are affected significantly both by the effect of polarization of the C_{60} cage by the outgoing photoelectron and encapsulation of H and He into the fullerene cage. The latter is specifically demonstrated by Figure 4d for enhanced clarity.

We now explore the angular dependence of the spin-polarization degree, $P_{j=\frac{1}{2}}(\theta)$, of the photoelectron fluxes from $C_{60}^-(2p)$, $H@C_{60}^-(2p)$ and $He@C_{60}^-(2p)$. We investigate $P_{j=\frac{1}{2}}(\theta)$ at two different values of the photoelectron momentum, k , where $\sigma_{2p \rightarrow s}$ significantly exceeds a fairly large $\sigma_{2p \rightarrow d}$. In photodetachment of $C_{60}^-(2p)$, this happens at $k \approx 0.485$ a.u. when polarizability of C_{60} is neglected ($\alpha = 0$) and at $k \approx 0.3$ a.u. in the case of $\alpha \neq 0$. Calculated $P_{j=\frac{1}{2}}(\theta)$, at $k = 0.485$ a.u., is depicted in Figure 5.

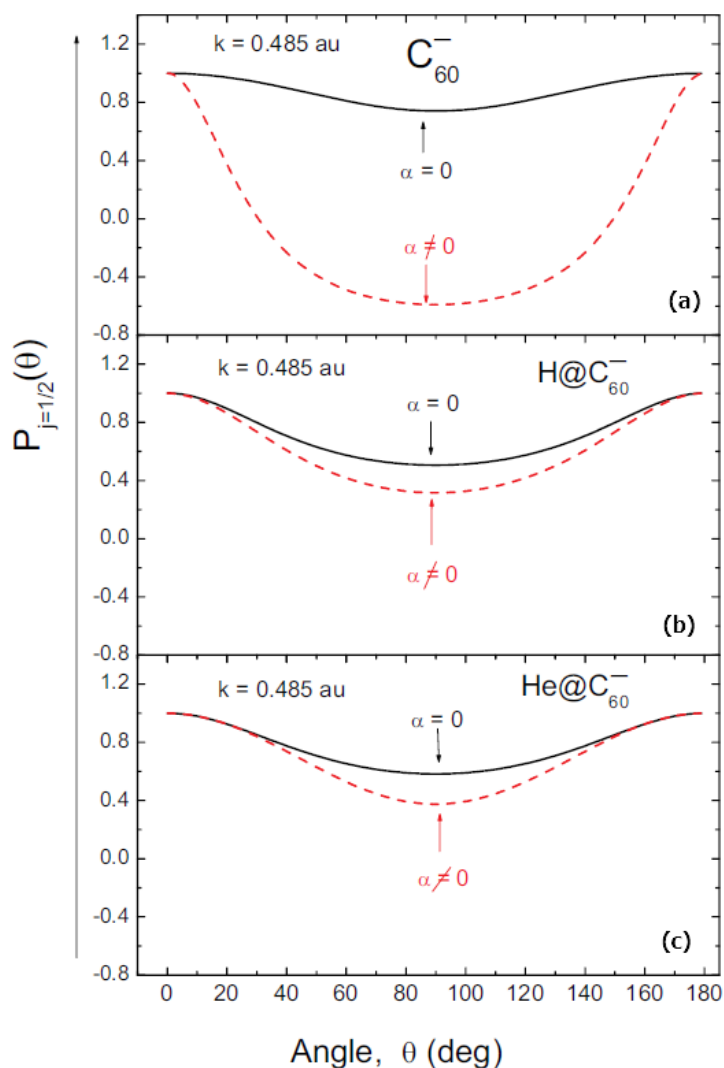


Figure 5. The angle-dependent degree of spin-polarization of photoelectron fluxes, $P_{j=\frac{1}{2}}(\theta)$, upon photodetachment of (a) $C_{60}^{-}(2p)$, (b) $H@C_{60}^{-}(2p)$ and (c) $He@C_{60}^{-}(2p)$ calculated at $k = 0.485$ a.u. without account ($\alpha = 0$) and with account ($\alpha \neq 0$) for polarization of the fullerene cage by the outgoing photoelectron, as marked.

Note how accounting for polarizability of C_{60} changes $P_{j=\frac{1}{2}}(\theta)$ for C_{60}^{-} dramatically, both quantitatively and qualitatively, including its sign change in a broad range of the emission angles, approximately from 30 to 150°. On the other hand, said polarization of the fullerene cage affects the spin-polarization degree of the photoelectrons from $H@C_{60}^{-}(2p)$ and $He@C_{60}^{-}(2p)$ significantly weaker. Moreover, the $P_{j=\frac{1}{2}}(\theta)$ s, calculated for $H@C_{60}^{-}(2p)$ and $He@C_{60}^{-}(2p)$, differ relatively little from each other. Hence, the angle-dependent degree of the photoelectron spin polarization is somewhat insensitive to the kind of an atom encapsulated inside the C_{60}^{-} cage, at least in the present case study.

Calculated $P_{j=\frac{1}{2}}(\theta)$ s, at $k = 0.3$ a.u., are plotted in Figure 6.

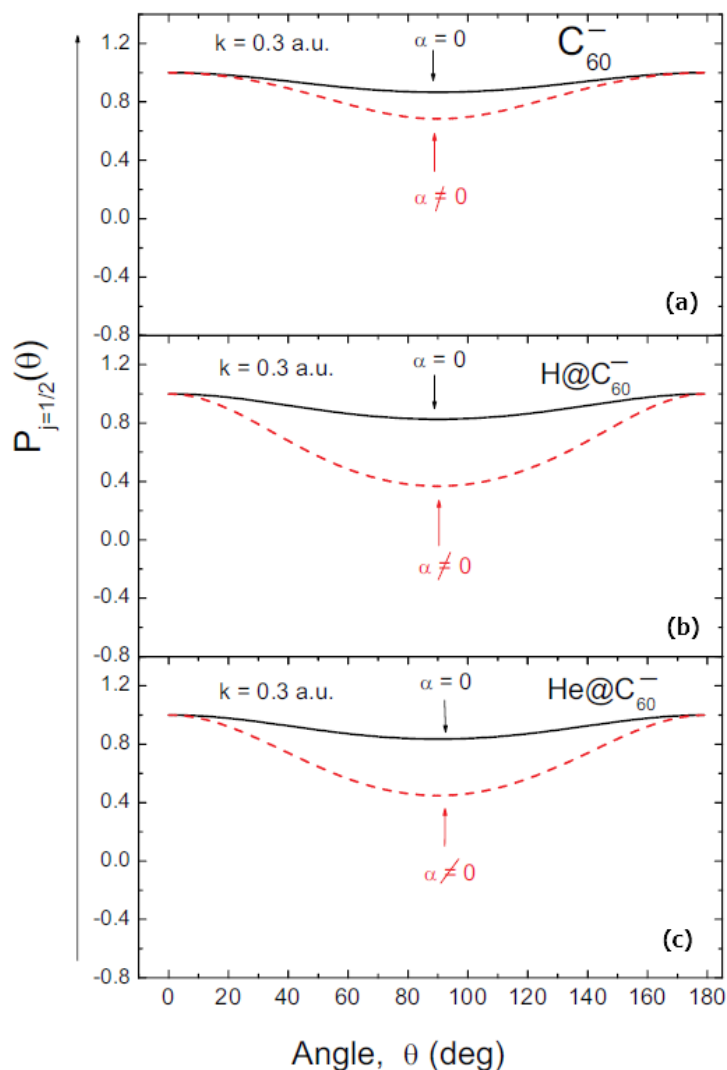


Figure 6. The angle-dependent degree of spin-polarization of the photoelectron fluxes, $P_{j=\frac{1}{2}}(\theta)$, upon photodetachment of (a) $C_{60}^{-}(2p)$, (b) $H@C_{60}^{-}(2p)$ and (c) $He@C_{60}^{-}(2p)$ calculated at $k = 0.3$ a.u. without account ($\alpha = 0$) and with account ($\alpha \neq 0$) for polarization of the fullerene cage by the outgoing photoelectron, as marked.

Overall, the behavior of $P_{j=\frac{1}{2}}(\theta)$ at $k = 0.3$ a.u. is similar to that of $P_{j=\frac{1}{2}}(\theta)$ at $k = 0.485$ a.u. It is similar in the respect that (a) accounting for polarizability of C_{60} only decreases the possible values of $P_{j=\frac{1}{2}}(\theta)$ regardless of the presence or absence of an atom inside C_{60}^{-} , (b) the encapsulation of an atom inside C_{60}^{-} results, overall, in decreased values of $P_{j=\frac{1}{2}}(\theta)$, and (c) the $P_{j=\frac{1}{2}}(\theta)$ s for the endohedral fullerene anions differ relatively little from each other. On a contrasting side, however, polarization of C_{60} by the outgoing photoelectron impacts $P_{j=\frac{1}{2}}(\theta)$ of empty $C_{60}^{-}(2p)$, at $k = 0.3$ a.u., only relatively insignificantly compared to the caused dramatic changes in $P_{j=\frac{1}{2}}(\theta)$ at $k = 0.485$ a.u.

4. Conclusions

In the present paper, we have provided a glimpse into spin-polarized photoelectron fluxes from fullerene anions. The key result is that photodetachment of fullerene anions may serve as a tool for producing highly spin-polarized photoelectron fluxes. This was shown to be due to a specific feature of photodetachment of fullerene anions—the presence of the domains of the photoelectron energies/momenta where a $d_{\ell-1}$ photodetachment amplitude exceeds by far a $d_{\ell+1}$ amplitude. Accounting for interactions omitted in the present study will likely change the details

of the reported results. However, it is unlikely that the omitted interactions would obliterate the very existence of the domains of the photoelectron momenta where the key inequality, $d_{\ell-1} \gg d_{\ell+1}$, takes place. Thus, the prediction of highly spin-polarized photoelectrons from fullerene anions should be qualitatively and semi-quantitatively accurate. It would be interesting to learn how the reported results would differ from those obtained in the framework of a rigorous theory. In this respect, let us stress once again that a similar simple model has been reasonably successful in the qualitative and quantitative description of experimental and other theoretical data on both the $4d$ photoionization of Xe@C_{60}^+ and differential elastic electron scattering off C_{60} .

Funding: This research received no external funding.

Conflicts of Interest: The author declares no conflict of interest.

Appendix A. Comparison of Calculated Data Obtained with the Use of $U_0 = 0.302$ and 0.347 a.u.

We demonstrate by Figure A1 that there are only insignificant differences between calculated $P_{2p}(r)$ radial wavefunctions, as well as $\sigma_{2p \rightarrow s}$, $\sigma_{2p \rightarrow d}$, β_{2p} , γ_1 and $P_{j=\frac{1}{2}}$ calculated with the use of $U_0 = 0.302$ and 0.347 a.u. for $U_C(r)$, Equation (9). Calculations were performed both with and without account for polarizability, α , of C_{60} . Thus, any of the potential depths fits, to a good approximation, to study spin-polarization photoelectron fluxes from fullerene anions.

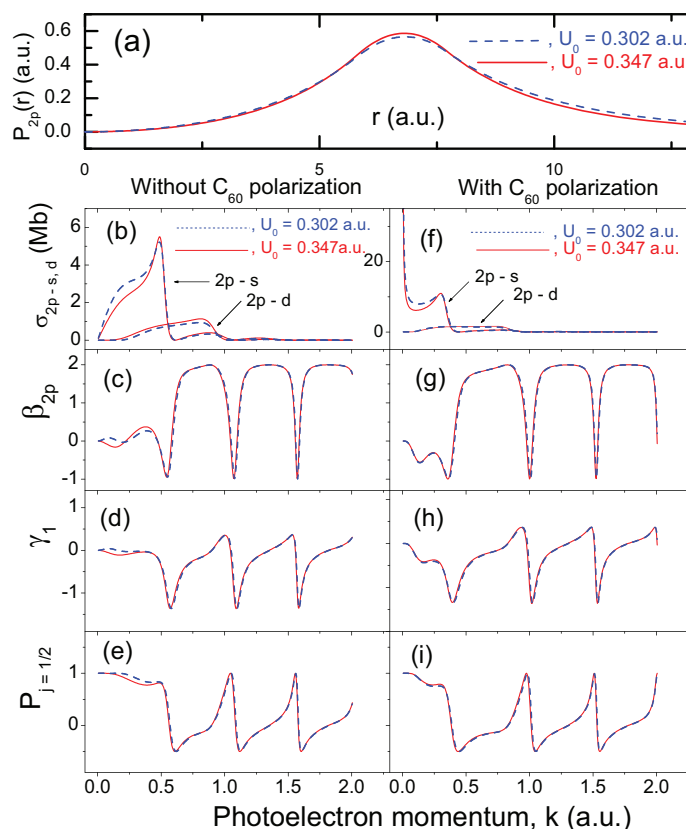


Figure A1. Calculated data for a $\text{C}_{60}^-(2p)$ anion obtained with the use of the depths $U_0 = 0.302$ a.u. (dashed lines) and 0.347 (solid lines) a.u. for the $U_C(r)$ pseudo-potential, Equation (9), as marked in the figure. (a) The $P_{2p}(r)$ radial part of the wavefunction of the attached $2p$ electron. (b–e) Calculated, without account for polarizability of C_{60} , $\sigma_{2p \rightarrow s}$ and $\sigma_{2p \rightarrow d}$ photodetachment cross sections, β_{2p} photoelectron angular-asymmetry parameter, γ_1 spin-polarization parameter and the $P_{j=\frac{1}{2}}$ angle-integrated degree of photoelectron spin polarization. (f–i) The same as (b–e) but with account for polarizability of C_{60} .

References

1. Kato, T. Absorption and emission spectra for C_{60} . *Laser Chem.* **1994**, *52*, 155. [[CrossRef](#)]
2. Bilodeau, R.C.; Gibson, N.D.; Walter, C.W.; Esteves-Macaluso, D.A.; Schippers, S.; Müller, A.; Phaneuf, R.A.; Aguilar, A.; Hoener, M.; Rost, J.M.; et al. Single-Photon Multiple Detachment in Fullerene Negative Ions: Absolute Ionization Cross Sections and the Role of the Extra Electron. *Phys. Rev. Lett.* **2013**, *111*, 043003. [[CrossRef](#)]
3. Müller, A.; Martins, M.; Kilcoyne, A.L.D.; Phaneuf, R.A.; Hellhund, J.; Borovik, A.; Holste, K.; Bari, S.; Buhr, T.; Klumpp, S.; et al. Photoionization and photofragmentation of singly charged positive and negative $Sc_3N@C_{80}$ endohedral fullerene ions. *Phys. Rev. A* **2019**, *99*, 063401. [[CrossRef](#)]
4. Lohr, L.L.; Blinder, S.M. Electron photodetachment from a Dirac bubble potential. A model for the fullerene negative ion C_{60}^- . *Chem. Phys. Lett.* **1992**, *198*, 100. [[CrossRef](#)]
5. Amusia, M.Y.; Baltenev, A.S.; Krakov, B.G. Photodetachment of negative C_{60}^- ions. *Phys. Lett. A* **1998**, *243*, 99. [[CrossRef](#)]
6. Korol, A.V.; Solov'yov, A.V. Vacancy decay in endohedral atoms: the role of an atom's non-central position. *J. Phys. B* **2011**, *44*, 085001. [[CrossRef](#)]
7. Baltenev, A.S.; Msezane, A.Z. Doubly-charged Negative Ion of C_{60}^- Molecule. *Proc. Dyn. Syst. Appl.* **2016**, *7*, 239.
8. Kumar, A.; Varma, H.R.; Deshmukh, P.C.; Manson, S.T.; Dolmatov, V.K.; Kheifets, A.S. Wigner photoemission time delay from endohedral anions. *Phys. Rev. A* **2016**, *94*, 043401. [[CrossRef](#)]
9. Chaudhuri, S.K.; Mukherjee, P.K.; Fricke, B. Spectroscopy of low lying transitions of He confined in a fullerene cage. *Eur. Phys. J. D* **2016**, *70*, 196. [[CrossRef](#)]
10. Dolmatov, V.K. Impact of fullerene polarizability on Wigner time delay in photodetachment of fullerene anions C_N^- . *J. Phys. Conf. Ser.* **2017**, *875*, 022013. [[CrossRef](#)]
11. Puska, M.J.; Nieminen, R.M. Photoabsorption of atoms inside C_{60} . *Phys. Rev. A* **1993**, *47*, 1181. [[CrossRef](#)] [[PubMed](#)]
12. Baltenev, A.S. Resonances in photoionization cross sections of inner subshells of atoms inside the fullerene cage. *J. Phys. B* **1999**, *32*, 2745. [[CrossRef](#)]
13. Scully, S.W.J.; Emmons, E.D.; Gharaibeh, M.F.; Phaneuf, R.A.; Kilcoyne, A.L.D.; Schlachter, A.S.; Schippers, S.; Müller, A.; Chakraborty, H.S.; Madjet, M.E.; et al. Photoexcitation of a volume plasmon in C_{60} ions. *Phys. Rev. Lett.* **2005**, *94*, 065503. [[CrossRef](#)] [[PubMed](#)]
14. Shields, D.; De, R.; Madjet, M.E.; Manson, S.T.; Chakraborty, H.S. Photoemission from hybrid states of $Cl@C_{60}$ before and after a stabilizing charge transfer. *J. Phys. B* **2020**, *53*, 125101. [[CrossRef](#)]
15. McCune, M.A.; De, R.; Madjet, M.E.; Chakraborty, H.S. First prediction of the direct effect of a confined atom on photoionization of the confining fullerene. *J. Phys. B* **2010**, *43*, 181001. [[CrossRef](#)]
16. McCune, M.A.; Madjet, M.E.; Chakraborty, H.S. Reflective and collateral photoionization of an atom inside a fullerene: Confinement geometry from reciprocal spectra. *Phys. Rev. A* **2009**, *80*, 011201(R). [[CrossRef](#)]
17. McCune, M.A.; Madjet, M.E.; Chakraborty, H.S. Unique role of orbital angular momentum in subshell-resolved photoionization of C_{60} . *J. Phys. B* **2008**, *41*, 201003. [[CrossRef](#)]
18. Dolmatov, V.K.; Edwards, A. Role of polarizability of a C_N fullerene cage in $A@C_N$ photoionization and $e^- - C_N$ scattering: the size effect. *J. Phys. B* **2019**, *52*, 105001. [[CrossRef](#)]
19. Baltenev, A.S.; Manson, S.T.; Msezane, A.Z. Jellium model potentials for the C_{60} molecule and the photoionization of endohedral atoms, $A@C_{60}$. *J. Phys. B* **2015**, *48*, 185103. [[CrossRef](#)]
20. Phaneuf, R.A.; Kilcoyne, A.L.D.; Aryal, N.B.; Baral, K.K.; Esteves-Macaluso, D.A.; Thomas, C.M.; Hellhund, J.; Lomsadze, R.; Gorczyca, T.W.; Ballance, C.P.; et al. Probing confinement resonances by photoionizing Xe inside a C_{60}^+ molecular cage. *Phys. Rev. A* **2013**, *88*, 053402. [[CrossRef](#)]
21. Gorczyca, T.W.; Hasoglu, M.F.; Manson, S.T. Photoionization of endohedral atoms using R-matrix methods: Application to $Xe@C_{60}$. *Phys. Rev. A* **2012**, *86*, 033204. [[CrossRef](#)]
22. Li, B.; O'Sullivan, G.; Dong, C. Relativistic R-matrix calculation photoionization cross section of Xe and $Xe@C_{60}$. *J. Phys. B* **2013**, *46*, 155203. [[CrossRef](#)]
23. Korol, A.V.; Solov'yov, A.V. Confinement resonances in the photoionization of endohedral atoms: Myth or reality? *J. Phys. B* **2010**, *43*, 201004. [[CrossRef](#)]

24. Amusia, M.Y.; Baltentkov, A.S.; Chernysheva, L.V.; Felfli, Z.; Msezane, A.Z. Dramatic distortion of the 4d giant resonance by the C₆₀ fullerene shell. *J. Phys. B* **2005**, *38*, L169. [[CrossRef](#)]
25. Dolmatov, V. On fullerene anions as sources of spin-polarized electrons. In Proceedings of the 12th European Conference on Atoms Molecules and Photons: Extended Abstracts (ECAMP 2016), Frankfurt am Main, Germany, 5–9 September 2016; p. 8.
26. Edwards, A.C.; Lane, C.G.; Dolmatov, V.K. Spin-polarized electrons upon nondipole photodetachment of fullerene anions. *J. Phys. Conf. Ser.* **2017**, *875*, 032032. [[CrossRef](#)]
27. Heinzmann, U.; Dil, J.H. Spin-orbit-induced photoelectron spin polarization in angle-resolved photoemission from both atomic and condensed matter targets. *J. Phys. B* **2012**, *24*, 173001. [[CrossRef](#)]
28. Dolmatov, V.K.; Amusia, M.Y.; Chernysheva, L.V. On the e⁻ – C₆₀ elastic angle-differential scattering cross section. *J. Phys. Conf. Ser.* **2020**, *1412*, 182011. [[CrossRef](#)]
29. Amusia, M.Y.; Chernysheva, L.V.; Dolmatov, V.K. Angle-differential elastic-electron scattering off C₆₀: A simple semi-empirical theory versus experiment. *J. Phys. B* **2019**, *52*, 085201. [[CrossRef](#)]
30. Tanaka, H.; Boesten, L.; Onda, K.; Ohashi, O. Cross-beam experiment for the scattering of low-energy electron from gas phase C₆₀. *J. Phys. Soc. Jpn.* **1994**, *63*, 485. [[CrossRef](#)]
31. Winstead, C.; McKoy, V. Elastic electron scattering by fullerene, C₆₀. *Phys. Rev. A* **2006**, *73*, 012711. [[CrossRef](#)]
32. Cherepkov, N.A. Angular distribution of photoelectrons with a given spin orientation. *Sov. Phys. JETP* **1974**, *38*, 463.
33. Cherepkov, N.A. Spin polarization of photoelectrons ejected from unpolarized atoms. *J. Phys. B* **1983**, *12*, 1279. [[CrossRef](#)]
34. Jaskólski, W. Confined many-electron systems. *Phys. Rep.* **1996**, *271*, 1. [[CrossRef](#)]
35. Buchachenko, A.L. Compressed atoms. *J. Phys. Chem. B* **2001**, *105*, 5839. [[CrossRef](#)]
36. Sabin, J.R.; Brändas, E.; Cruz, S.A. (Eds.) *Advances in Quantum Chemistry: Theory of Confined Quantum Systems. Part 1*; Academic: New York, NY, USA, 2009; Volume 57, pp. 1–334.
37. Sabin, J.R.; Brändas, E.; Cruz, S.A. (Eds.) *Advances in Quantum Chemistry: Theory of Confined Quantum Systems. Part 2*; Academic: New York, NY, USA, 2009; Volume 58, pp. 1–297.
38. Connerade, J.-P.; Kengkanb, P.; Semaounea, R. Confined Atoms in Clusters, Bubbles, Dots and Fullerenes. *J. Chin. Chem. Soc.* **2001**, *48*, 265. [[CrossRef](#)]
39. Connerade, J.-P. 2013 From Pauli's birthday to "Confinement Resonances" —A potted history of Quantum Confinement. *J. Phys. Conf. Ser.* **2013**, *438*, 012001. [[CrossRef](#)]
40. Sen, K.D. (Ed.) *Electronic Structure of Quantum Confined Atoms and Molecules*; Springer: New York, NY, USA, 2014; pp. 1–253.
41. Ley-Koo, E. Recent progress in confined atoms and molecules: Superintegrability and symmetry breakings. *Rev. Mex. Fis.* **2018**, *64*, 326. [[CrossRef](#)]
42. Chakraborty, H.S.; Deshmukh, P.C.; Manson, S.T. Interchannel-coupling effects in the spin polarization of energetic photoelectrons. *Phys. Rev. A* **2003**, *67*, 052701. [[CrossRef](#)]
43. Ivanov, V.K. Theoretical studies of photodetachment. *Radiat. Phys. Chem.* **2004**, *70*, 345. [[CrossRef](#)]
44. Amusia, M.Y.; Baltentkov, A.S. On the possibility of considering the fullerene shell C₆₀ as a conducting sphere. *Phys. Lett. A* **2006**, *360*, 294. [[CrossRef](#)]
45. Wang, L.-S.; Conceicao, J.; Jin, C.; Smalley, R.E. Threshold photodetachment of cold C₆₀⁻. *Chem. Phys. Lett.* **1991**, *182*, 5. [[CrossRef](#)]
46. Connerade, J.-P.; Dolmatov, V.K.; Manson, S.T. On the nature and origin of confinement resonances. *J. Phys. B* **2000**, *33*, 2279. [[CrossRef](#)]

